Spectrum of Engineering Sciences
ISSN (e) 3007-3138 (p) 3007-312X Volume 3, Issue 4, 2025

STRUCTURAL, THERMAL AND OPTICAL ANALYSIS OF Fe - DOPED NiO NANOPARTICLES FOR THERMOELECTRIC AND OPTOELECTRONIC APPLICATIONS

Awais Ur Rehman[*1], Ali Imam Haider[2], Safdar Khan[2], Muhammad Arshad Jamal[3], Salah Ud Din[4], Qamir Iqbal[5], Shah Wali Ullah[6], Muhammad Kashif Bashir[7], Muhammad Kashif Majeed[8]

[*1,2]*Department of Physics, Hazara University Mansehra, Pakistan*
[3,4]*Center of Excellence in Solid State Physics, University of the Punjab, Lahore, Pakistan*
[5]*School of Chemistry and Chemical Engineering, Department of Material Science, Shanxi University, China*
[6]*Advanced Functional Materials (AFM) Laboratory, Engineering Physics Department, Institute Technology Bandung, Bandung 40132, Indonesia*
[7]*Institute of Physics, the Islamia University of Bahawalpur, Pakistan*
[8]*School of Electronic Science and Technology, Xi'an Jiaotong University, Xi'an 710049, China. Faculty of Engineering Science and Technology, Iqra University, Karachi 75500, Pakistan*

[*1]awaisurrehmanphysicist@gmail.com, [2]alihaiderphy@gmail.com, [2]sardarsafdarzaman77@gmail.com, [3]raiarshadj@gmail.com, [4]salahmarri102@gmail.com, [5]mhrqamar602@gmail.com, [6]33323751@mahasiswa.itb.ac.id, [7]mkashifbashir624@gmail.com, [8]mkashif@iqra.edu.pk

DOI: https://doi.org/10.5281/zenodo.15227867

Keywords
Fe-doped NiO nanoparticles, Thermoelectric materials, Sol-gel synthesis, Optoelectronic applications.

Article History
Received on 08 March 2025
Accepted on 08 April 2025
Published on 16 April 2025

Corresponding Author: * Awais Ur Rehman[*1]

Abstract

This study is based on the structural, thermal and optical analysis of pure and Fe-doped NiO nanoparticles synthesized by the sol-gel method. At a calcined temperature of 500 ℃ for two hours, four samples (pure NiO, 2% Fe, 4% Fe, and 6% Fe doped NiO) have been prepared and characterized by X-ray diffraction (XRD), scanning electron microscopy (SEM), thermo gravimetric analysis (TGA) and UV-Visible spectroscopy. XRD confirms a single-phase FCC cubic structure with increasing average crystalline sizes of the particles, when the concentration of Fe increases. SEM reveals nanoparticles with increasing sizes, as Fe concentration increases the size of nanoparticles increases from 33.87nm (pure) to 63.89nm (6% Fe doped). TGA results show that less weight loss occurred in Fe-doped samples as compared to pure NiO; this led to enhanced thermal stability of prepared nanoparticles. The UV-visible result indicates red-shift with an increasing rate of absorption in the Fe-doped sample than in pure NiO. Also, the Tauc-Plot method shows that the shrinkage of energy band gap in Fe-doped samples, when compared to pure NiO sample. This study showed that doping of Fe in NiO enhances the structural, thermal and optical properties of the material. Iron-doped nickel oxide nanoparticles have the right structural, thermal, and optical properties to be used in thermoelectric and optoelectronic devices.

INTRODUCTION

Nanoparticle has been the subject of broad research since the beginning of their development because of their extraordinary real-world characteristics and bulk counterparts. Nano-scale materials are prepared in a number of ways [1]. Catalysts, photoelectric sensors, and recording materials are just a few of the applications of oxidized metals. These applications may be improved and controlled in a variety of ways by developing them into nanoscale materials. For the past few years, researchers have been focusing on them [2]. Metal oxide, also known as NiO, has fascinated mechanical and contemporary significance for its magnetic, electronic, mechanical, optical, and thermal properties. Due to its large band gap, this metal functions well as a P-type semiconductor [3]. Furthermore, in earlier research, NiO nanoparticles with various concentrations and iron annealing temperatures were examined, and it was observed that adding Fe to NiO NPs improves their characteristics and that they have remarkable magnetic, structural, and optical features. As a result of its excellent structural, optical, and magnetic characteristics, This material might be useful in a variety of applications, including optoelectronics, batteries, and sensors. [8]. A lot of work is being put into researching materials that will increase data storage in computers in the form of non-volatile memory in the future. This has inspired a wave of interest in the study of nanomaterials' appealing features, because they eventually allow electrical charge and spin to be controlled by changing the magnetic field [2]. Clearly, with zero applied fields, antiferromagnetic materials in bulk have no net magnetic moment, but magnificent particles of similar materials show either super-paramagnetic or fragile ferromagnetic material [4]. NiO is a transition metal oxide having a density of 6.67 grammas per cubic centimeter, a melting point of 1955 degrees Celsius, and an auto-ignition temperature of 400 degrees Celsius. NiO nanoparticles have a specific surface area of 130 to 150 nanometers and are measured between 10 and 30 nanometers. XRD analysis revealed that the NiO NPs have a face-centered cubic (FCC) crystal structure [10]. In the present study, we have synthesized Fe-doped NiO nanoparticles using the sol-gel method, a widely accepted technique due to its simplicity, cost-effectiveness, and ability to precisely control synthesis parameters such as temperature, pH, and precursor concentration. This method facilitates the formation of uniform particles with tunable morphology and crystallinity. The synthesized nanoparticles were subjected to comprehensive **structural, thermal, and optical analyses** to evaluate their suitability for **thermoelectric and optoelectronic applications**. The investigation aims to understand the influence of Fe doping on the structural phase, particle size, thermal stability, and optical band gap of NiO nanoparticles, thereby contributing to the advancement of multifunctional nanomaterials for next-generation devices. Despite the extensive research on nickel oxide (NiO) nanoparticles and their versatile applications in electronics, optics, and energy devices, several key areas remain underexplored. Although Fe doping has shown potential in enhancing the magnetic and optical properties of NiO, a comprehensive understanding of how iron incorporation influences the structural, thermal, and optical characteristics—specifically in the context of thermoelectric and optoelectronic applications—is still lacking.

Most existing studies focus either on the magnetic or catalytic properties of Fe-doped NiO, often overlooking the combined analysis of structural integrity, thermal stability, and band gap modulation, which are crucial parameters for energy-efficient and high-performance optoelectronic devices. Furthermore, there is limited comparative data on how varying Fe concentrations and synthesis parameters (such as annealing temperature and method) affect the functional properties of NiO at the nanoscale.

Additionally, while the sol-gel method is recognized for producing uniform nanoparticles, there is a need for more systematic investigations into how this technique can be optimized for Fe doping to fine-tune the material's multifunctional characteristics. The lack of detailed correlation between synthesis conditions, dopant concentration, and the resulting material properties represents a significant gap in the literature.

This study addresses these gaps by providing a thorough structural, thermal, and optical analysis of Fe-doped NiO nanoparticles synthesized via the sol-gel method, with the goal of identifying their

suitability and performance in thermoelectric and optoelectronic applications.

2 MATERIALS AND METHODOLOGY

2.1 Materials

The materials used in this research are: Nickel Nitrate Ni $(NO_3)_2$, Iron nitrate Fe $(NO_3)_3$, Ethanol and Sodium Hydroxide (NaOH). Distilled water was used in all the experimental procedures.

2.2 Preparation of pure and Iron doped NiO nanoparticles

In the course of this study, we prepared NPs consisting of both pure NiO and Fe- doped NiO by sol-gel method. In order to produce pure NiO NPs, we dissolved 3g of Nickel Nitrate Ni $(NO_3)_2$ in 30ml of distilled water. On the other hand, in order to produce iron-doped NiO, we added3g of Nickel Nitrate Ni $(NO_3)_2$ and 0.06g of iron nitrate Fe $(NO_3)_3$ to an aqueous solution that contained 30ml of distilled water. We stirred the solution for two hours to dissolve the salt completely. The salt solution was titrated by adding 0.5 M NaOH drop wise from burette with constant stirring. Frequently we checked the PH. The precipitates were formed when pH was 10. These precipitates were washed 4-5 times with ethanol and distilled water and then were dried at 150^0C for one hour to remove moisture. The dried material was grinded by mortar and pistil which resulted in 2% Fe doped NiO nanoparticles. In the end dried sample were calcined at 500^0C for 2 hours in a muffle furnace for removing the impurities in the product. Repeating the above procedure, we prepared 4% Fe doped NiO and 6% Fe doped NiO, for which we dissolved 0.12 g of iron nitrate Fe $(NO_3)_3$ and 0.18 g of iron nitrate Fe $(NO_3)_3$ with 3 g of nickel nitrate Ni $(NO_3)_2$ in 30 ml of distilled water, respectively. Experimental setup is displayed in figures 1 respectively.

2.3 Experimental setup of synthesized NPs

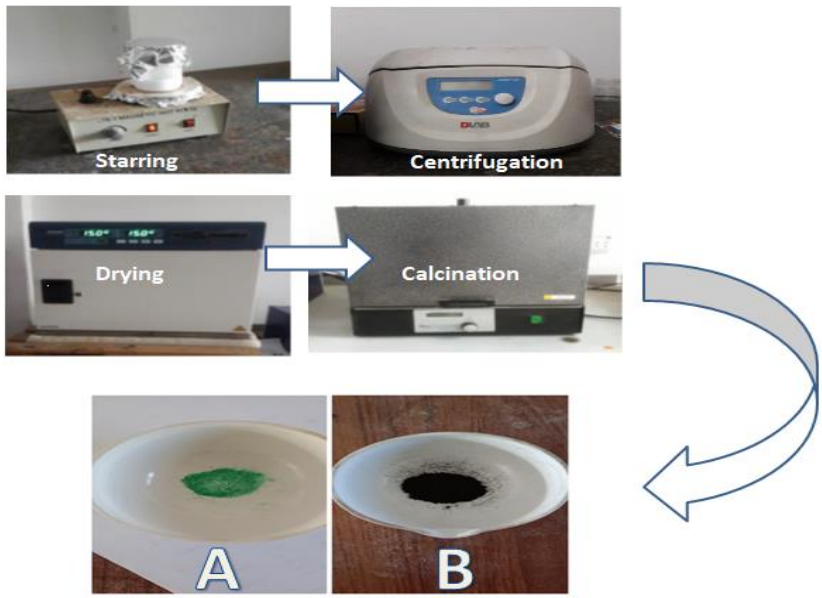

Figure 1: Experimental setup and synthesized Fe doped NiO nanopowder before (A) and after (B) calcinations.

3 RESULTS AND DISCUSSION

3.1 XRD analysis

According to XRD analysis, the structures of pure NiO and iron-doped NiO nanoparticles at concentrations of 2%, 4%, and 6% are shown in figure 2. From figure 2, in prepared nanoparticles, diffraction peaks have been detected at 36.35 °, 42.46 °, 62.32 °, and 74.79 °. Cubic FCC structure iron doped nickel oxide nanoparticles were found to have well-defined diffraction peaks (200), (111),

(220), (222) and (311) that match the standard spectrum (JCPDS, No.04-0835). The crystallinity of Fe-doped nanoparticles is demonstrated by the fine and sharp XRD peaks. According to the Scherrer equation, the average crystalline sizes obtained from diffraction ridges are 12.66 nm, 16.38 nm, 21.27 nm, and 29.15 nm for pure NiO, 2% Fe concentration, 4% Fe concentration, and 6% Fe concentration, respectively. Increased peak intensity indicates that crystallinity develops with doping and has a direct correlation to Fe concentration. The extremely small diffraction values of each sample produce a close correlation between the estimated crystalline sizes derived from Scherer's equation. By doping iron into nickel oxide, the average crystalline size increases from 12.66 nm to 29.15 nm. Ni^{+2}, Fe^{+2}, and Fe^{+3} have ionic radii of 0.69Å, 0.74 Å, and 0.64 Å, respectively. Due to the small difference in ionic radii between Ni^{+2}, Fe^{+2}, and Fe^{+3}, Fe-ions can substitute Ni^{+2} ions without compromising the lattice structure. Moreover, according to Pauling scale the electronegativity of both Ni and Fe cations are comparable (1.9 for Ni and 1.83 for Fe) thus Fe gets incorporated in to the NiO lattice at vacancy sites. The crystal sizes are listed in the table 1 below according to the dopant concentration.

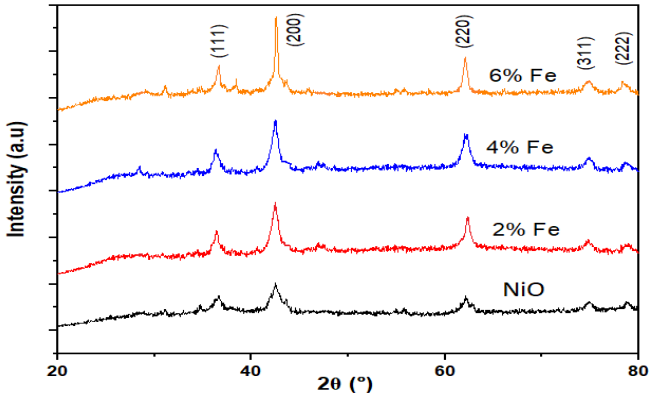

Figure 2: XRD patterns of pure and Fe- doped (2% Fe, 4% Fe and 6% Fe) NiO nanoparticles.

Table 1: Shows average crystalline sizes for pure NiO and Fe doped (2% Fe, 4% Fe and 6% Fe) NiO nanoparticles.

Concentration (%)	Average Crystallite Size (nm)
0 % Fe (pure NiO)	12.66 nm
2 % Fe-doped NiO	16.38 nm
4 % Fe-doped NiO	21.27 nm
6 % Fe-doped NiO	29.15 nm

3.2 SEM Analysis

SEM micrographs are used to determine the particle shape, size, and morphology of the sample. Figure 3 and 4 show SEM images of the produced Fe-doped NiO NPs for the samples. These images were obtained using a scanning electron microscope. Figure 3 displays four 0.5um SEM images taken at 50KX, with image A representing pure NiO, image B representing NiO with 2% Fe content, image C representing NiO with 4% Fe content, and image D representing NiO with 6% Fe content. In a similar manner, figure 4 displays four 1um SEM images taken at 15KX for pure NiO, 2% Fe doped NiO, 4% Fe doped NiO, and 6% Fe doped Nio, respectively. The images are labeled E, F, G, and H. These scanning electron micrographs SEM images demonstrate the morphology of Fe-doped NiO NPs. It has been noticed that the particles are agglomerated and nearly spherical and oval in shape, with a non-homogeneous distribution. The results of measuring the average particle sizes by image J software came out to be 33.87 nm, 45.07 nm, 53.35 nm, 63.89 nm for pure NiO, 2% Fe, 4% Fe and for 6% Fe respectively, which indicates that the size of the particles increases as the concentration of the Fe

increases. The table 2 below shows the particle sizes for pure and iron doped nickel oxide.

Table 2: Shows particle sizes for pure NiO and Fe doped (2% Fe, 4% Fe and 6%) NiO nanoparticles.

Samples	Particle size (nm)
Pure NiO	33.87
2% Fe-doped NiO	45.07
4% Fe- doped NiO	53.35
6% Fe-doped NiO	63.89

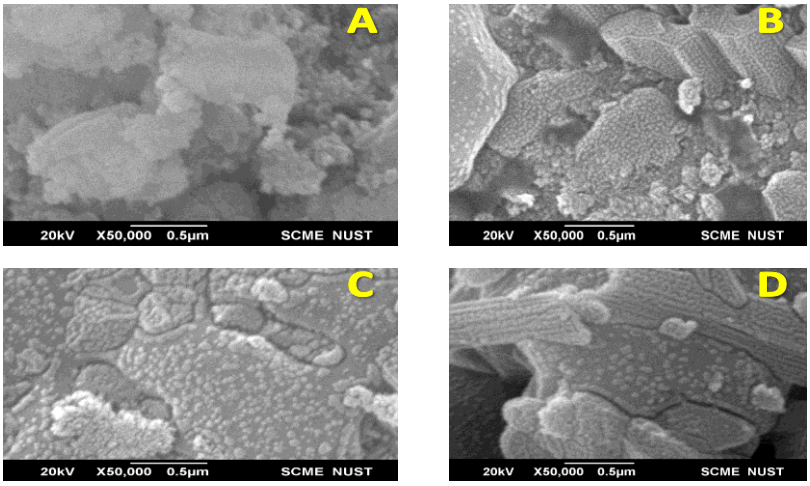

Figure 3: Shows four SEM images, image A representing pure NiO, image B representing NiO with 2% Fe doping, image C representing NiO with 4% Fe doping, and image D representing NiO with 6% Fe doping.

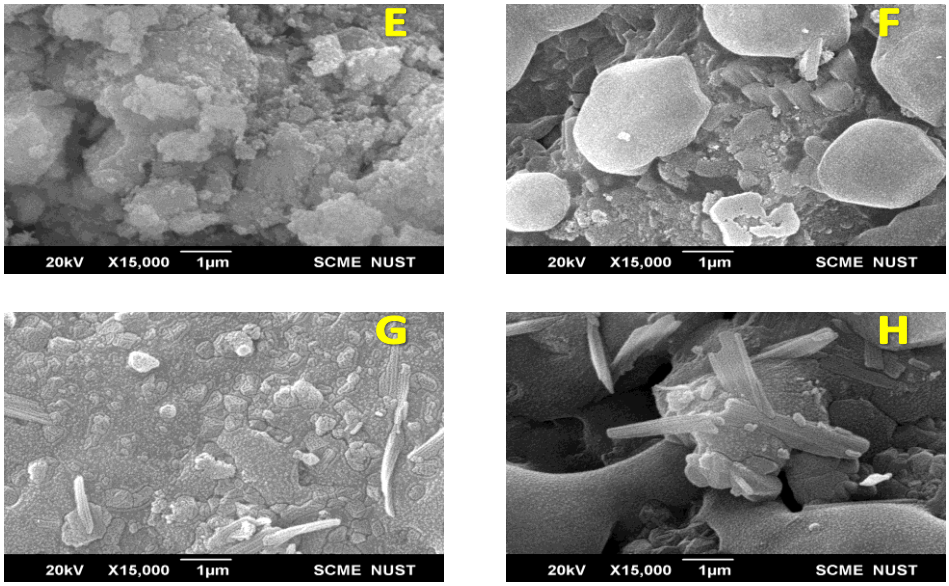

Figure 4: Shows four SEM images, image E representing pure NiO, image F representing NiO with 2% Fe doping, image G representing NiO with 4% Fe doping, and image H representing NiO with 6% Fe doping.

3.3 Thermal analysis

TGA determines changes in the weight of a sample in relation to a change in temperature. Thermal conductivity absorption spectroscopy (TGA) was used to record the TGA curves of the synthesized iron-doped and pure NiO from room temperature to 600°C with a heating rate of 5°C/min. All samples showed weight loss below 100°C, indicating the elimination of chemically adsorbed and structurally bonded water molecules.

3.3.1: Thermal analysis of pure NiO sample

Figure 5 below shows the TGA curve for pure NiO sample, a continuous weight loss of 0.3 mg was observed in the temperature range of 150°C to 350°C and 4 mg of weight loss was observed at temperature range of 500°C to 600°C, where 1.6 mg of total weight loss was observed up to 600°C.

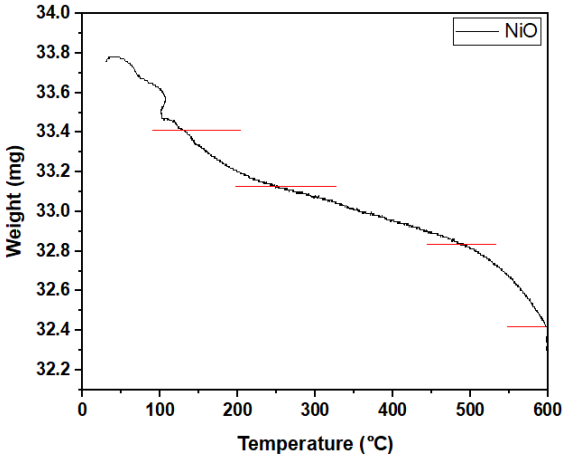

Figure 5: Shows TGA curve for pure NiO nanoparticles.

3.3.2 Thermal analysis of 2% Fe-doped NiO sample

Figure 6 below shows the TGA curve for 2% Fe-doped NiO sample, in which a continuous weight loss of 0.27 mg was observed in the temperature range of 140°C to 250°C and 0.3 mg of weight loss observed at a temperature of 500°C to 600°C where 1.1 mg of total weight loss was observed up to 600°C for this sample. The total weight loss of this sample is reduced as compare to the total weight loss of pure NiO, this shows that 2% Fe-doped NiO sample is more stable than pure NiO up to 600°C.

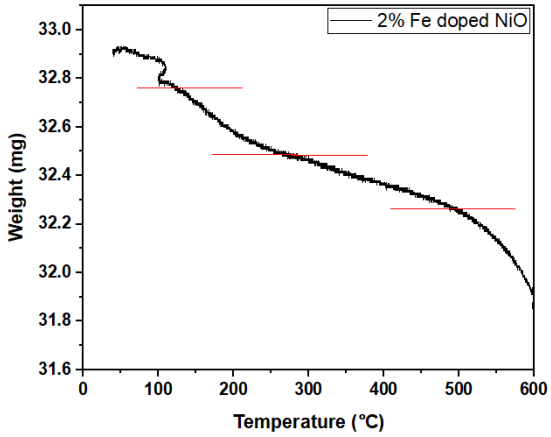

Figure 6: Shows TGA curve for 2% Fe doped NiO nanoparticles.

3.3.3 Thermal analysis of 4% Fe-doped NiO sample

Figure 7 below shows the TGA curve for 4% Fe-doped NiO sample in which a continuous weight loss of 0.27 mg was observed in the temperature range of 160°C to 240°C and 0.25 mg of weight loss at a temperature of 500°C to 600°C, while 1 mg of total weight loss was observed up to 600°C for this simple, which is lower than pure and 2% Fe doped NiO. This indicates that 4% Fe doped NiO sample is more stable than pure and 2% Fe doped NiO up to 600°C.

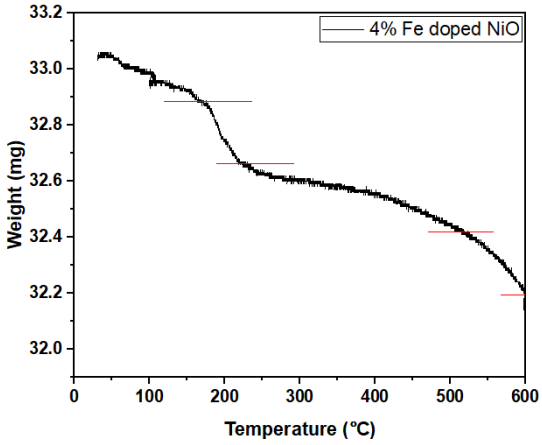

Figure 7: Shows TGA curve for 4% Fe doped NiO nanoparticles.

3.3.4 Thermal analysis of 6% Fe-doped NiO sample

Figure 8 below shows the TGA curve for 6% Fe doped NiO sample in which a continuous weight loss of 0.7 mg was observed at 425°C to 600°C where 0.9 mg of total weight loss was observed up to 600°C. The total weight loss of this sample is lower in comparison with 2% Fe, 4% Fe and with pure NiO. And it is also observed that pure, 2% and 4% Fe-doped nickel oxide decomposes earlier than 6% Fe doped nickel oxide and is consistent over the temperature range, indicating that 6% Fe-doped nickel oxide is more stable than 2%, 4% and pure nickel oxide. The first stage of weight loss in all samples is may be due to oxidation of Ni^{+2} or Fe^{+2} to higher oxidation state where the second stage of weight loss may be due to the decomposition of an unstable or off stoichiometric. As validated the EDX data synthesized nanoparticles are either nearly stoichiometric or slightly oxygen rich. Due to the nanoparticles' thermal stability, no further weight loss was detected in all samples. As the amount of Fe increases in NiO, it is seen that the samples lose less weight as the temperature increases. The table 3 below listed the percentage of total weight loss up to 600°C for pure NiO and Fe doped (2% Fe, 4% Fe and 6% Fe) NiO nanoparticles.

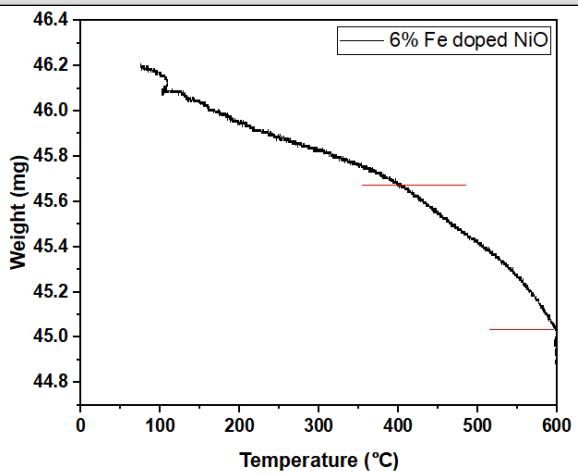

Figure 8: Shows TGA curve for 6% Fe doped NiO nanoparticles.

Table 3: Showing the weight loss in percentage for pure and Fe doped (2% Fe, 4% Fe and 6% Fe) NiO nanoparticles.

3.5: UV-Vis Analysis

The optical absorption spectra of pure and doped (2% Fe, 4% Fe, and 6% Fe) NiO nanoparticles are shown in figure 9. As seen in the spectra, the absorption edges of all doped samples with increasing rate of absorption are significantly red-shifted relative to the absorption edge of pure NiO. This results in the formation of nanoparticles. Furthermore, band gap graphs, using well-known Tauc plots method are shown in figure 10, of the synthesized nanoparticles. From figure 10, it is evident that band gap become shrinkage by adding Fe in NiO nanoparticles. And it is also observed that as Fe concentration increases, the band gap of the nanoparticles decreases. Since NiO is a p-type material, it is expected that holes will accumulate near the top of the valence band as a result of Fe doping, which may result in band gap contraction as in our case. This leads to improved optical characteristics of the material.

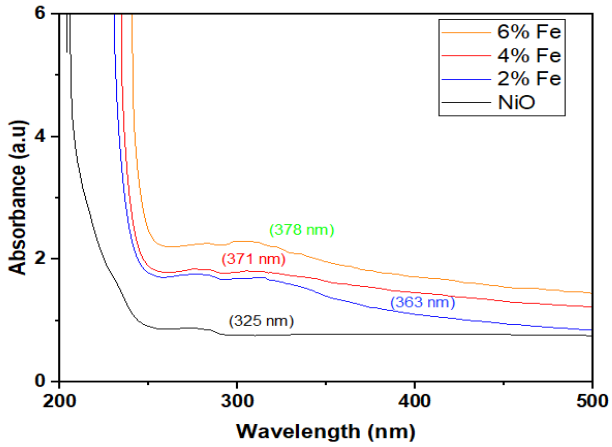

Figure 9: Absorption spectra of pure and Fe doped (2% Fe, 4% Fe and 6% Fe) NiO nanoparticles.

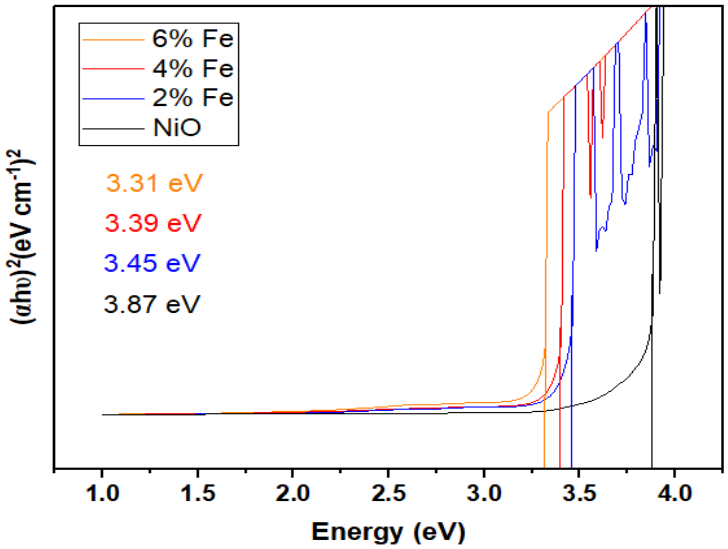

Figure 10: Direct band gap energies spectra of pure and Fe doped (2% Fe, 4% Fe and 6% Fe) NiO nanoparticles.

Samples	Total weight (mg)	weight loss (mg)	Weight loss percentage (%)
Pure NiO	34.0	1.6	4.70
2% Fe doped NiO	33.0	1.1	3.33
4% Fe doped NiO	32.2	1	3.10
6% Fe doped NiO	46.6	1.4	3.00

Table 4: Band gap energies for pure and Fe doped (2% Fe, 4% and 6%) NiO nanoparticles.

Samples	Direct band gap energies (eV)
Pure NiO	3.87
2% Fe	3.45
4% Fe	3.39
6% Fe	3.31

Conclusion

Pure and iron-doped (2%, 4%, and 6%) NiO naoparticles have been successfully synthesized at a calcined temperature of 500^{0}C for two hours by a simple and low-cost process called sol-gel. XRD confirms the cubic FCC structure with an increase in crystalline size from 12.66 nm (pure) to 29.15 nm (6% Fe-doped) . SEM analysis reveals nanoparticles with increasing size from pure NiO to 6% Fe doped NiO. Size of the nanoparticles increases with increasing Fe concentration. TGA analysis shows that the slight increase in weight loss for pure NiO sample with increasing temperatures in comparison with 2%, 4% and 6% Fe doped NiO samples. And it is also observed that the weight loss of the Fe doped NiO samples reduces with increasing Fe concentration. The UV-Visible analysis revealed a red shift in the absorption spectrum and reduction in band gap with the increasing Fe concentration for direct band gap.

REFERENCES

Benelmekki, M. An introduction to nanoparticles and nanotechnology. In Designing Hybrid Nanoparticles. Morgan & Claypool Publishers, 2015.

Sudha, P. N., Sangeetha, K., Vijayalakshmi, K., &Barhoum, A. Nanomaterials history, classification, unique properties, production and market. In Emerging Applications of Nanoparticles and Architecture Nanostructures (pp. 341- 384). Elsevier, 2018.

Jeevanandam, J. Barhoum, A., Chan, Y. S., Dufresne, A., &Danquah, M. K. Review on nanoparticles and nanostructured materials: history, sources, toxicity and regulations. Beilstein journal of nanotechnology, 9(1), 1050-1074, (2018).

Pokropivny, V., Lohmus, R., Hussainova, I., Pokropivny, A., &Vlassov, S. Introduction to nanomaterials and nanotechnology (pp. 45-100). Ukraine: Tartu University Press, (2007).

Dolez, P.I. Nanomaterials definitions, classifications, and applications. In Nanoengineering (pp. 3-40). Elsevier, (2015).

Khan, W. S., & Asmatulu, R.. Nanotechnology emerging trends, markets, and concerns. In Nanotechnology safety (pp. 1-16), Elsevier. (2013).

Kumar, S. K., &Krishnamoorti, R. Nanocomposites: structure, phase behavior, and properties. Annual Review of Chemical and Biomolecular Engineering, 1, 37-58, (2010).

Mody, V. V., Siwale, R., Singh, A., &Mody, H. R.. Introduction to metallic nanoparticles. Journal of Pharmacy and Bioallied Sciences, 2(4), 282, (2010).

Nagarajan, R., "Nanoparticles: Building Blocks for Nanotechnology", ACS Symposium Series, Washington, pp. 1-14, 2008.

Rakesh, R. "Nanotechnology", S. Chand and Company Ltd, India, pp. 37, Chap 1. 2009.

Gleiter, H. "Nanostructured Materials: State of the Art and Perspectives", Nanostructured Materials, 6, pp. 3-14, 1995.

Nalwa, H. S., , "Handbook of Nanostructured Materials and Nanotechnology", Academic Press, Elsevier Inc, Japan, pp. 1-2, Chap. 1, 2000.

Papaefthymiou, G. C., , "Nanoparticle Magnetism", Nano Today, 4, pp. 438-447, 2009 .

Siegel, R. W., "Nanostructured Materials Mind Over Matter", Nanostructured Materials, 3, pp. 1-18, 1993.

Siegel, R. W., , "Nanophase Materials Assembled from Atom Clusters", Materials Science and Engineering: B, 19, pp. 37-43, 1993 .

Pelecky, D. L. L., and Rieke, R. D., "Magnetic Properties of Nanostructured Materials", Chemistry of Materials, 8, pp. 1770-1783, 1996.

Bonder, M. J., Huang, Y., and Hadjipanayis, G. C., , "Advanced Magnetic Nanostructures", Springer, New York, USA, pp. 183-186, Chap. 7, 2006.

Fernandez, C. D. J., "Influence of the Temperature Dependence of Anisotropy on the Magnetic Behavior of Nanoparticles", Physical Review B: Condensed Matter and Materials Physics, 72, pp. 054438, 2005.

Brauer, B., Vaynzof, Y., Zhao, W., Kahn, A., Li, W., Zahn, D. R. T., Fernandez, C. D. J., Sangregorio, C., and Salvan, G., , "Electronic and Magnetic Properties of Ni Nanoparticles Embedded in Various Organic Semiconductor Matrices", The Journal of Physical Chemistry B, 113, pp. 4565-4570, 2009.

Li, Q., Wang, L. S., Hu, B. Y., Yang, C., Zhou, L., and Zhang, L., , "Preparation and Characterization of NiO Nanoparticles through Calcination of Malate Gel", 61, pp. 1615-1618, 2007.

An, Z., Pan, S., and Zhang, J., "Facile Preparation and Electromagnetic Properties of Core-Shell Composite Spheres Composed of Aloe-like Ni Flowers Assembled on Hollow Glass Spheres", The Journal of Physical Chemistry C, 113, pp. 2715-2721, 2009 .

Jia, B. F., Zhang, L., Shang, X., and Yang, Y., "Non-Aqueous Sol-Gel Approach Towards the Controllable Synthesis of Ni Nanospheres, Nanowires and Nanoflowers", Advanced Materials, 20, pp. 1050-1054, 2008.

Liu, B. Z., Li, S., Yang, Y., Peng, S., Hu, Z., and Qian, Y., "Complex-Surfactant-Assisted Hydrothermal Route to Ferromagnetic Ni Nanobelts", Advanced Materials, 15, pp. 1946-1948, 2003.

Cordente, N., Respaud, M., Senocq, F., Casanove, M. J., Amines, C., and Chaudret, B., "Synthesis and Magnetic Properties of Ni nanorods", Nano Letters, 1, pp. 565-568, 2001.

Couto, G. G., Klein, J. I., Schreiner, W. H., Mosca, D. H., Oliveira, A. J. A. D., and Zarbin, A. J. G., "Nickel Nanoparticles Obtained by a Modified Polyol Process: Synthesis, Characterization and Magnetic Properties", Journal of Colloid and Interface Science, 311, pp. 461-468, 2007.

Ni, X., Zhao, Q., Zhang, D., Zhang, X., and Zheng, H., "Novel Hierarchial Nanostructures of Nickel: Self-Assembly of Hexagonal Nanoplatelets", The Journal of Physical Chemistry C, 111, pp. 601-605, 2007.

Zhang, G., Zhang, T., Lu, X., Wang, W., Qu, J., and Li, X., , "Controlled Synthesis of 3D and 1 D Nickel Nanostructures Using an External Magnetic Field Assisted Solution-Phase Approach", The Journal of Physical Chemistry C, 111, pp. 12663-12668, 2007.

Niu, H., Chen, Q., Ning, M., Jia, Y., and Wang, X., "Synthesis and One-Dimensional Self-Assembly of Acicular Nickel NanocrystallitesUnder Magnetic Fields", The Journal of Physical Chemistry B, 108, pp. 3996-3999, 2004.

Leng, Y., Yan, L., Li, X., and Takahashi, S. "Improved Magnetic Anisotropy of Monodispersed Triangular Nickel Nanoplates", The Journal of Physical Chemistry C, 111, pp. 6630-6633, 2007.

Leng, Y., Zhang, Y., Liu, T., Suzuki, M., and Xingguo, L."Synthesis of Single Crystalline Triangular and Hexagonal Ni Nanosheets with Enhanced Magnetic Properties", Nanotechnology, 17, pp. 1797-1800, 2006.

Zhang, D., Ni, X., and Zheng, H."Surfactant-Controlled Synthesis of Fe Nanorods in Solution", Journal of Colloid and Interface Science, 292, pp. 410-412, 2005.

Park, S. J., Kim, S., Lee, S., Khim, Z. G., Char, K., and Hyeon, T."Synthesis and Magnetic Studies of Uniform Iron Nanorods and Nanospheres", Journal of the American Chemical Society, 122, pp. 8581-8582, 2000.

Peng, S., Wang, C., Xie, J., and Sun, S."Synthesis and Stabilization of Monodisperse Fe Nanoparticles", Journal of the American Chemical Society, 128, pp. 10676-10677, 2006.

Joseyphus, R. J., Shinoda, K., Kodama, D., and Jeyadevan, B."Size Controlled Fe Nanoparticles ThroughPolyol Process and their Magnetic Properties", Materials Chemistry and Physics, 123, pp. 487-493, 2010.

Jafari, T., Simchi, A., and Khakpash, N. "Synthesis and Cytotoxicity Assessment of Superparamagnetic Iron-Gold Core-Shell Nanoparticles Coated with Polyglycerol", Journal of Colloid and Interface Science, 345, pp. 64-71, 2010.

N.N.M. Zorkipli, N.H.M. Kaus, A.A. Mohamad, "Synthesis of NiO Nanoparticles through Sol-gel Method," Procedia Chemistry, 19, 626–631, 2016.

M.S. Alshatwi, H.A. Alburaih, S.S. Alghamdi, D.A. Alfadhil, J.A. Alshehri, F.A. Aljamaan "Iron-doped Nickel Oxide Nanoparticles Synthesis and Analyzing Different Properties", Advances in Science, Technology and Engineering Systems Journal, vol. 6, no. 1, pp. 1422-1426 , 2021.

P. Jeevanandam, V.R.R. Pulimi, "Synthesis of nanocrystallineNiO by solgel and homogeneous precipitation methods," Indian Journal of Chemistry - Section A Inorganic, Physical, Theoretical and Analytical Chemistry, 51, 586–590, 2012.

M. Alagiri, S. Ponnusamy, C. Muthamizhchelvan, "Synthesis and characterization of NiO nanoparticles by sol–gel method," Journal of Materials Science-Materials in Electronics - J MATER SCI-MATER ELECTRON, 23, 2012.

P. Mallick, C. Rath, R. Biswal, N.C. Mishra, "Structural and magnetic properties of Fe doped NiO," Indian Journal of Physics, 83, 517–523, 2009.

Ahmed, Abdullah Ahmed Ali, Enas Ali Ahmed Alahsab and Abdullah Mohamed Abdulwahab. "The influence of Zn and Mg doping on the structural and optical properties of NiOnano-structures for optoelectronic applications." Results in physics 22, 2021.

K.N. Patel, M.P. Deshpande, V.P. Gujarati, S. Pandya, V. Sathe, S.H. Chaki, "Structural and optical analysis of Fe doped NiO nanoparticles synthesized by chemical precipitation route," Materials Research Bulletin, 106, 187–196, 2018.

P.M. Ponnusamy, S. Agilan, N. Muthukumarasamy, T.S. Senthil, G. Rajesh, M.R. Venkatraman, D. Velauthapillai, "Structural, optical and magnetic properties of undopedNiO and Fe-doped NiO nanoparticles synthesized by wet-chemical process," MaterialsCharacterization,114(C),166–171,2016.

H. Abbas, K. Nadeem, A. Hassan, S. Rahman, H. Krenn, "Enhanced photocatalytic Activity of Ferromagnetic Fe-doped NiO nanoparticles," Optik, 202, 163637, 2020.

R. Pradeep, A.C. Gandhi, Y. Tejabhiram, I.K.M.M. Sahib, Y. Shimura, L. Karmakar, D. Das, S.Y. Wu, Y. Hayakawa, "Magnetic anomalies in Fedoped {NiO} nanoparticle," Materials Research Express, 4(9), 96103, 2017.

Fominykh K, Chernev P, Zaharieva I, Sicklinger J, Stefanic G, Döblinger M, Müller A, Pokharel A, Böcklein S, Scheu C, Bein T, Fattakhova-Rohlfing D. Iron-doped nickel oxide nanocrystals as highly efficient electrocatalysts for alkaline water splitting. ACS Nano. May 26;9(5):5180-8, 2015.

Bayappagari, B., Shaik, K., Chakraborty, D. et al. Structural, optical and magnetic properties of vacuum annealed Fe, Mn doped NiO nanoparticles. Appl. Phys. A 127, 49 2021.

Hur Abbas, K. Nadeem, S. Munir, U. Ahmed, M. Usman, Mikhail Kostylev, Fe–Co co-doping effects on antiferromagnetic core of NiO nanoparticles, Ceramics International, Volume 48, Pages 3435-3447, Issue 3, 2022.

Iimori, T., Imamoto, Y., Uchida, N., Kikuchi, Y., Honda, K., Iwahashi, T. and Ouchi, Y.Magnetic moment distribution in nanosized antiferromagnetic NiO. Journal of Applied Physics, 127(2), p.023902, 2020.

M.H. Mamat, N. Parimon, A.S. Ismail, I.B. ShameemBanu, S. SathikBasha, R.A. Rani, A.S. Zoolfakar, M.F. Malek, A.B. Suriani, M.K. Ahmad, M. Rusop,Synthesis, structural and optical properties of mesostructured, X-doped NiO (x = Zn, Sn, Fe) nanoflake network films,Materials Research Bulletin, Volume 127, 2020.

Sharma, Ratnesh&Acharya, Aman&Shrivastava, S.B. &Patidar, Manju&Gangrade, Mohan &Shripathi, Thoudinja&Ganesan, V... Studies on the structure optical and electrical properties of Zn-doped NiO thin films grown by spray pyrolysis. Optik - International Journal for Light and Electron Optics, (2016).

Kandpal, NarainDatt, NeetiSah, RenuLoshali, Rajendra P. Joshi and J. Sarada Prasad. "Co-precipitation method of synthesis and characterization of iron oxide nanoparticles." 2014.

Mishra, D., Arora, R., Lahiri, S. et al. Synthesis and characterization of iron oxide nanoparticles by solvothermal method. Prot Met PhysChem Surf 50, 628–631, 2014.

Absi, Eman&Saleh, Muneer& Al-Hada, Naif Mohammed &Hamzah, Khaidzir&Alhawsawi, Abdulsalam&Banoqitah, Essam. Correction to: A review on preparation and characterization of silver/nickel oxide nanostructures and their applications. Applied Physics A. 127, 2021.

Anand, G. Theophil, R. Nithiyavathi, R. Ramesh, S. John Sundaram, and K. Kaviyarasu. "Structural and Optical Properties of Nickel Oxide Nanoparticles: Investigation of Antimicrobial Applications." Surfaces and Interfaces 18, 2020.

kalangestani, F.C., Simiari, M. &Ghodsi, F.E. Preparation and characterization of vanadium-doped nickel oxide nanostructure deposited by dip-coating technique. Eur. Phys. J. Plus 136, 517, 2021.

M. Niederberger and N. Pinna, Metal Oxide Nanoparticles in Organic Solvents: Synthesis, Formation, Assembly and Application (Engineering Materials and Processes), Springer, Berlin, Germnay, 2009.

Feinle, M. S. Elsaesser, and N. Hüsing, "Sol-gel synthesis of monolithic materials with hierarchical porosity," Chemical Society Reviews, vol. 45, no. 12, pp. 3377–3399, 2016.

Y. Liao, Y. Xu, and Y. Chan, "Semiconductor nanocrystals in sol-gel derived matrices," Physical Chemistry Chemical Physics, vol. 15, no. 33, Article ID 13704, 2013.

G. J. Owens, R. K. Singh, F. Foroutan et al., "Sol-gel based materials for biomedical applications," Progress in Materials Science, vol. 77, pp. 1–79, 2016.

M. Haruta, "Nanoparticulate gold catalysts for low-temperature CO oxidation," Journal of New Materials for Electrochemical Systems, vol. 7, pp. 163–172, 2004.

G. AdaikalaSelvan, S. Rachel, T. Gajendran, Chapter 13 - Several assorted characterization methods of nanoparticles, Editor(s): R. Praveen Kumar, B. Bharathiraja, Nanomaterials, Academic Press, Pages 301-308, 2021.

Mahmoud Nasrollahzadeh, MonirehAtarod, MohaddesehSajjadi, S. Mohammad Sajadi, Zahra Issaabadi, Chapter 6 - Plant-Mediated Green Synthesis of Nanostructures, journal of colloidal and interface science, 2016.

Mechanisms, Characterization, and Applications, Editor(s): Mahmoud Nasrollahzadeh, S. Mohammad Sajadi, MohaddesehSajjadi, Zahra Issaabadi, MonirehAtarod, Interface Science and Technology, Elsevier, Volume 28, Pages 199-322, 2019.

Macdonald, G. Puzzles: Morrison Formation, **Starting Point**.from,http://serc.carleton.edu/introgeo/interactive/examples/morrisonpuzzle.html.Retrieved Sept9,2004.

Argast, Anne and Tennis, Clarence F. A web resource for the study of alkali feldspars and perthitic textures using light microscopy, scanning electron microscopy and energy dispersive X-ray spectroscopy, Journal of Geoscience Education 52, no. 3, p. 213-217, 2004.

Beane, Rachel, Using the Scanning Electron Microscope for Discovery Based Learning in Undergraduate Courses, Journal of Geoscience Education, vol 52 #3, p. 250-253, 2004.

James Gomes, JyotiBatra, Viki R. Chopda, P. Kathiresan, Anurag S. Rathore, Chapter 25 - Monitoring and Control of Bioethanol Production From Lignocellulosic Biomass, Editor(s): ThalladaBhaskar, Ashok Pandey, S. Venkata Mohan, Duu-Jong Lee, Samir Kumar Khanal, Waste Biorefinery, Elsevier, , Pages 727-749, 2012.

Lokesh Kumar, Md. ShahnwajAlam, ChhuttanLalMeena, Rahul Jain, Arvind K. Bansal, Chapter 4 - Fexofenadine Hydrochloride, Editor(s): Harry G. Brittain, Profiles of Drug Substances, Excipients and Related Methodology, Academic Press, Volume 34, Pages 153-192, ISSN 1871-5125, 2009.

Walter F. da Silva Júnior, Jonas G. de Oliveira Pinheiro, Carlos D.L.F.A. Moreira, Fabia J.J. de Souza, Ádley A.N. de Lima, Chapter 15 - Alternative Technologies to Improve Solubility and Stability of Poorly Water-Soluble Drugs, Editor(s): Alexandru Mihai Grumezescu, Multifunctional Systems for Combined Delivery, Biosensing and Diagnostics, Elsevier, Pages 281-305, 2017.

Rakhee, Jigni Mishra, Raj K. Sharma, KshipraMisra, Chapter 9 - Characterization Techniques for Herbal Products, Editor(s): KshipraMisra, Priyanka Sharma, AnujaBhardwaj, Management of High Altitude Pathophysiology, Academic Press, , Pages 171-202, 2018.